Cationic distribution in the new Nd₂CaSnO₆ perovskite type-phase

Noureddine Boudar [1], Abderrahim Aatiq [1,*], Hajar Bellefqih [1], Asmaa Marchoud [1], Bouchaib Manoun [2] and Brahim Orayech [3]

[1] University Hassan II of Casablanca, Faculty of Sciences Ben M'Sik, Chemistry Department. Laboratory of Physical-Chemistry of Applied Materials, Avenue Idriss El Harti, B.P. 7955, Casablanca, Morocco

[2] University Hassan I, Faculté des Sciences et Technique de Settat, Laboratoire des Sciences des Matériaux, Morocco

[3] CIC EnergiGune, Power Storage; Batteries and Supercaps, Albert Einstein, 48, 01510 Miñano, Alava, Spain.

Abstract: The new Nd₂CaSnO₆ double perovskite oxide has been synthesized in polycrystalline form by a conventional solid-state reactions process at 1300°C in air atmosphere. Structure refinement, realized by Rietveld analysis using the X-ray powder diffraction (XRD) data, shows that the compound crystallizes in monoclinic symmetry with $P2_1/n$ space group and $Z = 2$. Obtained unit-cell parameters are: a = 5.6585(1) Å, b = 5.9254(1) Å, c = 8.1883(2) Å, β = 90.116(1) ° and $V = 274.5(1)$ Å³. The cationic distribution over the A- and *B*-sites of this perovskite structure can be illustrated by the $[Nd_{1.90}Ca_{0.10}]_A[Nd_{0.10}Ca_{0.90}]_{B'}[Sn_{1.00}]_{B''}O_6$ crystallographic formula. The monoclinic structural distortion involves long-range ordering between Sn^{4+} (in 2c site) and a random mixture $(_{0.90}Ca^{2+}; _{0.10}Nd^{3+})$ (in 2d site) all at the B-perovskite sites.

Keywords: Double perovskite; X-Ray diffraction; Crystal structure; Rietveld refinement; Cationic distribution.

Introduction

Perovskite oxides ABO₃ can be described as the framework of corner-shared BO₆ octahedra with 12-coordinated A cation. When two different cations are introduced at the B site, double perovskite structures with the formula of $A_2B'B''$O₆ are formed. Compounds crystallizing in this structure-family are among the most intensely studied materials in solid state chemistry and physics. They exhibit several fundamentally interesting chemical and physical properties [1-6]. The wide range of interesting properties stems largely from the exceptional structural and compositional flexibility of the perovskite structure.

To understand the physical properties of the $A_2B'B''$O₆ double perovskites, it is important to know the arrangement and position of the $B'(B'')$ cations because the B cations generally determine the physical properties of perovskites ABO₃. It should be noticed that differences in size and charge of the B-site cations lead to three types of arrangements; random, rocksalt arrangement when the cations alternate in all three dimensions and occasionally, the B' and B'' cations may also form a layered order, where they alternate only in one direction [7]. Schematic structures are shown in Figure 1. In this scheme rock salt, columnar and layered ordering become (111), (110) and (001) ordering, respectively.
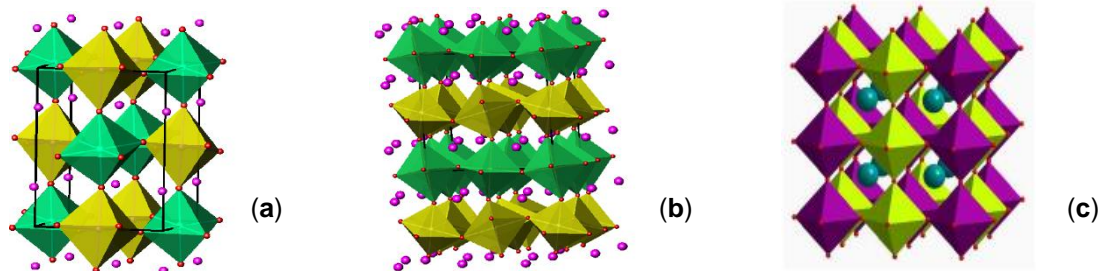

Figure 1. The crystal structures of perovskite with rock-salt (a) layered (b) and columnar (c) octahedral *B*-cation ordering.

According to several reports, in double perovskite materials containing rare earth ions, the nature and the size of the other elements of the material, seems to be the force driving of selective occupancy of their *A* and *B* sites. Thereby in the case of La_2CuTiO_6, the Cu^{2+} and Ti^{4+} ions are distributed randomly in the *B*-sites (*Pnma* space group) [8] however M^{2+} (*M*=Zn, Mg) and Ti^{4+} ions in La_2MTiO_6 and Nd_2MgTiO_6 show that cations in B sites are arranged in the rock salt configuration (*P2₁/n* space group) (Figure 1a) [9-11]. Structures of Ln_2CuSnO_6 (Ln = Pr, Nd, Sm) double perovskite [7,12] show a layered distribution of *B*-cations similar to that observed for La_2CuSnO_6 (*P2₁/m* space group) [13] (Figure 1b). The large differences of ionic radii and oxidation state between Ca^{2+} and Sb^{5+}, result in the ordering distribution of Ca^{2+} and Sb^{5+} cations within *B*-sites of Ca_2LaSbO_6 and Ca_2NdSbO_6 (*P2₁/n* space group) [14-17]. Cationic distribution of both compounds can be illustrated respectively by the $[CaLa]_A[CaSb]_BO_6$ [15-16] and $[CaNd]_A[CaSb]_BO_6$ [17] crystallographic formula [15-17]. Similar cationic distribution are also found in the $[Ca_{1/3}La_{2/3}]_A[Ca_{1/3}Ti_{2/3}]_BO_3$ compound (*P2₁/n* space group) [18]. It should be pointed out that in the case of Ca_2SmSbO_6 and Ca_2LnRuO_6 (Ln=La-Lu) phases (*P2₁/n* space group) a peculiar cationic distribution have been reported [14,16]. Indeed, the Ca^{2+} and Ln^{3+} cations are partially disordered in the *A* and *B'* sites positions of the $A_2B'B''O_6$ perovskite phase; the Ru^{5+} and Sb^{5+} occupied only the *B''* sites. Their crystallographic formulas have been written as $[Ca_{(2-x)}Ln_x]_A[Ln_{(1-x)}Ca_x]_{B'}[M]_{B''}O_6$ (M = Ru, Sb). In our previous structural characterization study of $[Ca_{1/3}Ln_{2/3}]_A[Cu_{1/3}Ti_{2/3}]_BO_3$ (Ln = Pr, Nd, Sm) and $[Ca_{1/3}Ln_{2/3}]_A[Zn_{1/3}Ti_{2/3}]_BO_3$ (Ln = La, Pr, Nd, Eu) phases, some of us have shown the existence of a statistical cationic distribution within the *A* and *B* sites of the perovskite (*Pbnm* space group) [19,20]. As shown by the crystallographic formula, in all materials the rare earth cation occupied only the A sites. In a continuation of our scientific research, herein, we report the structure as well as the cationic distribution within both *A* and *B*-sites of the Nd_2CaSnO_6 double perovskite.

Material and Methods

Polycrystalline Nd_2CaSnO_6 was prepared by classical high temperature solid-state chemistry from powdered mixtures of Nd_2O_3, $CaCO_3$ and SnO_2 in the adequate stoichiometric ratio. The mixture was heated progressively with intermittent grinding at 900°C (12 h), 1000°C (24 h), pressed into pellets and sintered at 1300°C for another 48 h in air atmosphere. The sample was cooled to room temperature for re-grinding several times. The compound was characterised by X-ray diffraction (XRD) at room temperature with a Panalytical X′Pert-PRO (*θ-2θ*) diffractometer equipped with x'celerator detector; (Cu*Kα*) radiation (45 kV, 40 mA); divergence slit of 1°, receiving slit of 0.10 mm, and antiscatter slit of 1°. The data were collected from 10 to 90° 2θ, in steps of 0.02°, with a counting time of 15 s per step. The Rietveld refinement of the structure was performed using the Fullprof program [21].

Results and Discussion

Structural refinement

In a first time, the obtained XRD of Nd_2CaSnO_6 shows that his structural refinement can be performed in the space group *Pbnm* (a non standard setting of *Pnma*) based on a similar orthorhombic $GdFeO_3$ type-structure with a randomly cationic distribution within the *A* and *B* site of the ABO_3 perovskite [22]. The atomic position of $GdFeO_3$were used as starting parameters for the Rietveld refinement of Nd_2CaSnO_6. Our attempt to refine the structure of Nd_2CaSnO_6 using a structural model with the *Pbnm* space group was not successful because some experimental diffraction lines (e.g., diffraction peak at around $2\theta = 18.47°$) are not generated (Figure 2a). Since the experimental XRD pattern of Nd_2CaSnO_6 also has diffraction peaks from a small amount (about 6 wt. %) of the $Nd_2Sn_2O_7$, the Rietveld refinement was carried out using a two-phase model, consisting of Nd_2CaSnO_6 and $Nd_2Sn_2O_7$. It should be noted that only high-intensity diffraction peaks of $Nd_2Sn_2O_7$ appear as impurity in the XRD pattern. In order to explain the splitting of some diffraction lines in the XRD spectra of Nd_2CaSnO_6, it was necessary to find a structural model with a lower symmetry than the orthorhombic. Analyzing the different structural models expected in the case of double-perovskite structures, we found that the model with the *P2₁/n* space group could explain all features of the diffraction profile. Also, we observed that the systematic absences of the reflections h0l with h+l=2n+1 and 0k0 with k=2n +1 in the XRD powder pattern suggests the space group *P2₁/n*. As it will be shown later, the presence of 0kl: k = 2n+1 reflection (e.g., reflection (011) at $2\theta \sim 18.47°$) is evidence that the B-cation arrangement is rock salt and not random. Note that many reports show that both *A* and *B* sites, in the ABO_3 perovskite, can be occupied either by calcium and/or Neodymium atoms as it was mentioned for example in $Ca(Ca_{1/3}Nb_{2/3})O_3$ [23-24] and Ca_2NdSbO_6 (i.e. $[CaNd]_A[CaSb]_BO_6$) [17]. It is well known that Sn^{4+} ($r_{VI Sn}^{4+} = 0.69$ Å) ion prefer to occupy the octahedral *B*-site of ABO_3 perovskite.

Concerning the Ca^{2+} and Nd^{3+} cations, we note that there is no significant difference between their ionic radii in octahedral *B*-site (i.e., $r_{VI Nd}^{3+} = 0.98$ Å, $r_{VI Ca}^{2+} = 1.00$ Å) but for the *A*-site, and if we consider a twelve coordination, a relatively significant difference between their ionic radii ($r_{XII Nd}^{3+} = 1.27$ Å, $r_{XII Ca}^{2+} = 1.34$ Å) is observed [25]. According to the last remarks it is difficult to distribute, without ambiguity, the Ca and Nd atoms in Nd_2CaSnO_6 between the two *A* and *B*-sites of the perovskite structure. In order to clarify the cationic distribution in Nd_2CaSnO_6, the structural refinement was realized in three principal steps. In the first step, starting parameters for the

Rietveld refinement of Nd_2CaSnO_6 were based on those reported for Nd_2MgTiO_6 ($P2_1/n$ space group) [11]. The Ca and Sn atoms were constrained to be distributed between the two possible 2d (½ 0 0)

position (i.e., *B'* type-site) and 2c (0 ½ 0) position (i.e., B'' type-site) and the Nd atoms are supposed the reside only in the *A*-sites of the perovskite (i.e: 4e (x y z) positions).
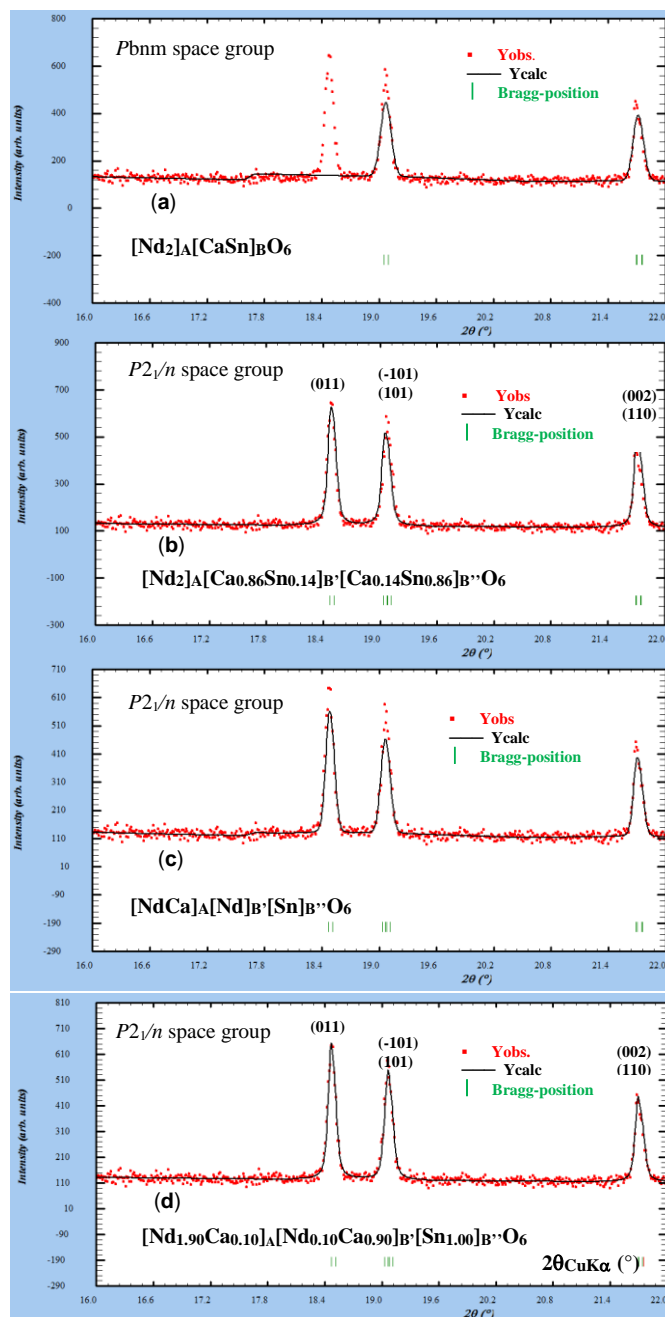

Figure 2. Experimental (●●●) and calculated (—) of the XRPD patterns, in the 16-22 ($2\theta°$) range (Cu$K\alpha$ radiation), of Nd_2CaSnO_6. Bars in green (│) indicate the Bragg peak positions. Results of the Rietveld refinement is given for each hypothesis of cationic distribution and the allowed reflections are also reported.

The occupancy factors for Ca and Sn atoms within the two possible positions were allowed to vary, but the total cation contents were constrained to be in accordance with the stoichiometry of the initial synthesized mixture. Obtained cationic distribution can be illustrated by the $[Nd_2]_A[Ca_{0.86}Sn_{0.14}]_{B'}$-

$[Ca_{0.14}Sn_{0.86}]_{B''}O_6$ crystallographic formula. As shown in the Figure 2b, the concordance between experimental and calculated XRD data is not

satisfactory but, as already predicted, this last result shows a high tendency for Sn atoms to occupy the 2c position of the octahedral site. This refinement leads also to a negative value for the displacement parameters of Ca and Sn in 2d and 2c sites. In fact, the negative values for the displacement parameters of Ca and Sn suggest an electronic deficit within the 2d and 2c sites. Although the results of this refinement are not too satisfactory, they clearly show the necessity of assuming the distribution of a heavier atom than Ca

and Sn in perovskite B sites. In fact, given that Nd_2CaSnO_6 contains Neodymium atoms, which have a relatively high atomic number (i.e., $Z_{Nd} = 60$), in the next refinement step, the Rietveld refinement with the hypothesis of $[NdCa]_A[NdSn]_BO_6$ crystallographic formula was tested. During this last refinement one Nd and Sn atoms are distributed between the two 2d and 2c positions of the *B*-sites while the Calcium and the other Neodymium atom has been localized within the A-sites (i.e.: 4e (~0.51 ~0.55 ~0.25) position). This refinement leads to relatively larger values of reliability factors [e.g., R_B =7%]. Experimental and calculated XRD from this Rietveld refinement, over the 2θ range from 16° to 22°, are compared in Figure 2c with results obtained from the previous other hypotheses of cationic distribution. During the final step of refinement, the Sn atoms are localized in the 2c position (i.e., *B''* type site) while the occupancy rate of Nd and Ca atoms, within the 4e (i.e., *A*-sites) and 2d position of *B'*-sites (i.e., (½ 0 0)), have been allowed to vary but the total Nd and Ca atoms contents were constrained to be in accordance with the stoichiometry of compound. Surprisingly, this refinement led to acceptable reliability factors, e.g., R_B = 3.8%. Thereby the final obtained cationic distribution that satisfactorily reproduces all the characteristics of the pattern (i.e., $[Nd_{1.90}Ca_{0.10}]_A[Nd_{0.10}Ca_{0.90}]_{B'}[Sn_{1.00}]_{B''}O_6$

crystallographic formula) is different from that normally expected. In fact, we need to distribute the Nd^{3+} cation between the *A* and *B'*-sites; otherwise the model is not able to correctly reproduce the experimental intensity of many peaks in the pattern. It should be noticed that for a given *B* cation radius (or *B'B''* combination average of $A_2B'B''O_6$), there is an ideal *A* cation size, as defined by a tolerance factor *t* equal to 1 (i.e.: $t = \dfrac{rA + rO}{\sqrt{2}\,(r\bar{B} + rO)}$, where the $r\bar{B}$ is the mean radius of *B'* and *B''*, r_A and r_O are respectively the ionic radii of *A* and O atoms) [26], where the *A* cation perfectly fits the cubic network of corner-sharing octahedra. When the *A* cation size is smaller, and the tolerance factor becomes less than 1, an octahedral tilting distortion typically occurs to reduce the effective coordination number of the *A* cation and consequently leads to a decrease of the number of its neighbours oxygen's from twelve to eight. Given that the ionic radius of eight coordinate for Ca^{2+} ($r_{VIII\,Ca^{2+}}$ = 1.12 Å) is only 0.01 Å greater than that of Nd^{3+} ($r_{VIII\,Nd^{3+}}$ = 1.11 Å) [25], the obtained cationic distribution which is illustrated by the final crystallographic formula $[Nd_{1.90}Ca_{0.10}]_A[Nd_{0.10}Ca_{0.90}]_{B'}[Sn_{1.00}]_{B''}O_6$, can be explained by the fact that the Ca^{2+} cation has displaced the Nd^{3+} cation from the *A*-site position of the double perovskite.
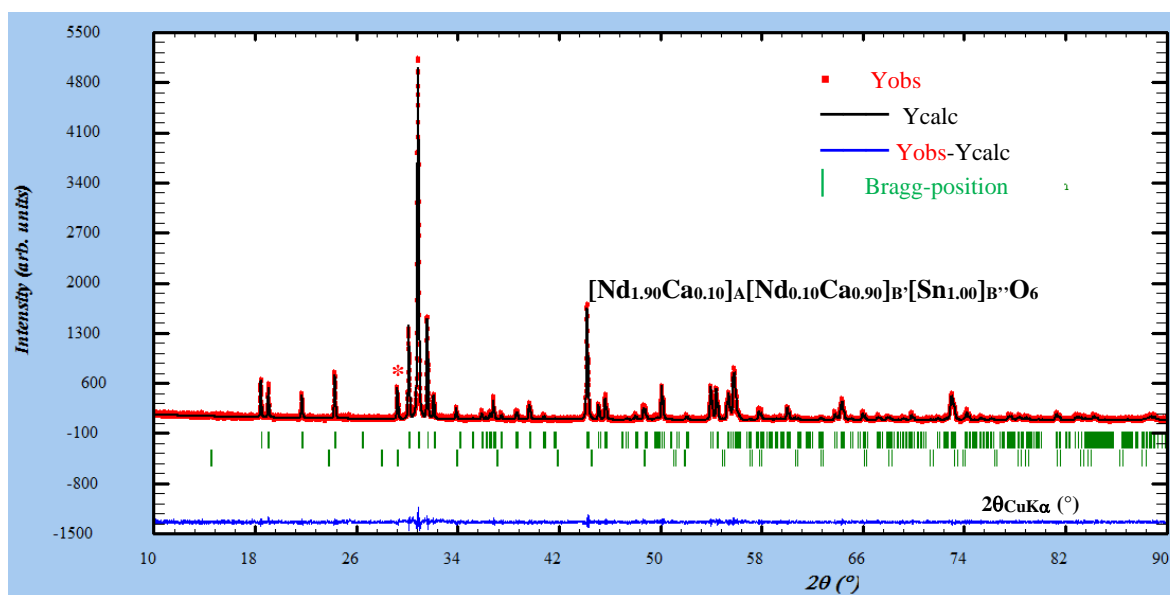

Figure 3. Experimental (●●●) calculated (—), and difference profile (—) of the XRPD patterns of Nd_2CaSnO_6 ($CuK\alpha$ radiation). Bars in green (|) indicate the Bragg peak positions. The top bars correspond to Nd_2CaSnO_6 whereas the bottom bars correspond to $Nd_2Sn_2O_7$. The main peaks corresponding to the $Nd_2Sn_2O_7$ phase are indicated by asterisk (*).

Experimental and calculated XRD from the final step of Rietveld refinement are also compared in Figure 2d, over the 2θ range from 16° to 22°, with the previous results. It should be noticed that during the last Rietveld analyses the displacement parameters of atoms, within the two *B'* and *B''* sites, were constrained to be equal and the oxygen sublattice was assumed to be fully occupied. The agreement between

the observed and calculated profile of the final Rietveld refinement, in the 10-90° (2θ -range), of Nd_2CaSnO_6 is shown in Figure 3.

The results of refinement, the atomic positions, selected bonds distances, bond valence sums [27] and bond angles are summarized in Tables 1-3. X-ray data, obtained from the ''observed intensities'' of the

Rietveld refinement (Cu$K\alpha1$: 1.5406 Å), of Nd_2CaSnO_6 are given in Table 4.

Structural Description

Structure of Nd_2CaSnO_6 phase consists of three types of polyhedra, $(Nd_{1.90}, Ca_{0.10})(1)O_{12}$, $(Ca_{0.90}, Nd_{0.10})(2)O_6$ and SnO_6 (Figure 4). $(Nd_{1.90}, Ca_{0.10})(1)$ cations are statistically distributed within the A-site of $[Nd_{1.90}Ca_{0.10}]_A[Nd_{0.10}Ca_{0.90}]_{B'}[Sn_{1.00}]_{B''}O_6$ compounds whereas the $(Ca_{0.90}, Nd_{0.10})(2)$ cations occupied the B' type site. The type of *B*-cations ordering results in a partially ordered structure with alternating $\{111\}_c$ plane occupied exclusively by Sn^{4+} cations (2c site) and a random mixture $(Ca_{0.90},Nd_{0.10})(2)$, in 2d site, of $Ca^{2+}(2)$ and the remaining $Nd^{3+}(2)$ cations (Figure 4). The average $< (Ca, Nd)_B$-O$>$ distance (2.296 Å) in $(Ca_{0.90}, Nd_{0.10})(2)O_6$ Octahedra is significantly larger than that for Sn-O bonds (2.050 Å) in SnO_6 as expected from the difference between the six-coordinated radii of $(Ca_{0.90}, Nd_{0.10})(2)$ (0.998 Å) and Sn^{4+} (0.69 Å). Octahedral B'-sites are regular whereas the B''-sites are therefore slightly distorted (Table 2).

Table 1. Results of the Rietveld refinement of Nd_2CaSnO_6.

Nd_2CaSnO_6 ($[Nd_{1.90(2)}Ca_{0.10(2)}]_A[Nd_{0.10(2)}Ca_{0.90(2)}]_{B'}[Sn_{1.00}]_{B''}O_6$ crystallographic formula)
Space group: $P2_1/n$; [Z = 2, a = 5.6585(1) Å, b = 5.9254(1) Å, c = 8.1883(2) Å; β = 90.116(1)° V = 274.5(1) Å³]
Experimental data
Temperature, 298 K ; angular range, 10° ≤ 2θ ≤ 100°; step scan increment (2θ), 0.01°
Zero point (2θ), -0.012(1)°
Profile parameters:
Pseudo-voigt function, PV = ηL + (1-η)G; η = 0.712(2)
Half-width parameters, U = 0.038(2), V= -0.012(2) and W = 0.0059(1)
Conventional Rietveld R-factors, R_{WP} = 8.9%; R_P = 6.8%; R_B = 3.8%; R_F = 4.2%

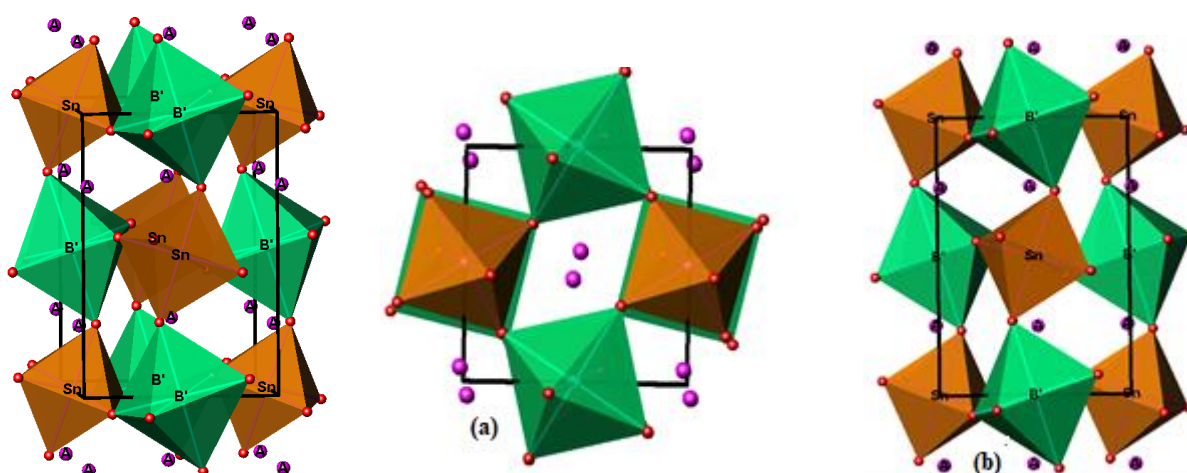| Atom	Site	Wyckoff positions			B_{iso}(Å²)	Occupancy
Nd(1)	4e	0.5161(4)	0.5579(2)	0.2479(3)	0.79(5)	0.95(1)
Ca(1)	4e	0.5161(4)	0.5579(2)	0.2479(3)	0.79(5)	0.05(1)
Ca(2)	2d	0.5	0	0	0.58(2)	0.45(1)
Nd(2)	2d	0.5	0	0	0.58(2)	0.05(1)
Sn	2c	0	0.5	0	0.054(7)	0.50
O(1)	4e	0.1711(2)	0.2058(2)	-0.0713(2)	0.60(1)	1
O(2)	4e	0.2989(2)	0.6730(2)	-0.0547(2)	0.60(1)	1
O(3)	4e	0.3837(2)	0.9482(2)	0.2663(2)	0.60(1)	1

Figure 4. Crystal structure of a double perovskite in the $P2_1/n$ space group showing views down the (a) 110 and (b) 001 directions highlighting the a−a−c+ tilt system used to model each of the reported structures. Red spheres correspond to O sites for a given $[Nd_{1.90}Ca_{0.10}]_A[Nd_{0.10}Ca_{0.90}]_{B'}[Sn_{1.00}]_{B''}O_6$.

These octahedra are rotated around a twofold axis parallel to [110] and a fourfold axis parallel to [001] of the aristotype phase. As a consequence of these rotations the coordination number of $(Nd, Ca)_A$ cations has changed from 12 to 8. In fact, if we consider the first coordination sphere, which includes only cation to oxygen bonds with a distance smaller than the shortest *A* site to B-site bond distance (i.e., *A-B'* = 3.315(2) Å), the $(Nd, Ca)_A$ cations within the A-site are eight coordinated (Table 2). It should be pointed out that the percent order, in Nd_2CaSnO_6, can be evaluated from the occupancy parameters obtained by the Rietveld refinements analysis. In fact, zero percent order would have 50% each of *B'* and *B''* on

each of the octahedral sites of the $A_2B'B''O_6$ double perovskite. For 100% order, there would be 100% of B' on the B' site and 100% B'' on the B'' site. For intermediate degrees of order, the degree of cation ordering, within B-sites, is quantified with the long range order parameter abbreviated by (LRO). The expression of LRO is LRO = $[2\times(Occ.)_B-1]\times100$ where $(Occ.)_B$ is the fractional occupancy of the B' or the B'' cation on the octahedral site that is predominantly occupied by that cation [28-29]. Given that in $[Nd_{1.90}Ca_{0.10}]_A[Nd_{0.10}Ca_{0.90}]_{B'}[Sn_{1.00}]_{B''}O_6$, the B'' sites are fully occupied by Sn atoms, the LRO parameter of Nd_2CaSnO_6 can be evaluated only based

on the occupancy for cations in the B'-sites. Since the B' site contain 90% of Ca^{2+} (Table 1), the obtained value of LRO parameter is $[2\times0.90-1]\times100 = 80\%$. Bond valence sum of the A-site cation which includes only the first coordination sphere (eight A-O bonds) agree with the ideal value (Table 2). Note that the slight divergence between observed and calculated bond valence sums, of B-site cations, can be related to the disordered distribution of the two atom types within the same crystallographic B' site. Structural data indicate a symmetric coordination environment for the B-site ions and nearly comparable B'-O and B''-O bond distances are observed (Table 2).

Table 2. Selected interatomic distances (Å) for Nd_2CaSnO_6.

$([Nd_{1.90(2)}Ca_{0.10(2)}]_A[Nd_{0.10(2)}Ca_{0.90(2)}]_{B'}[Sn_{1.00}]_{B''}O_6$ crystallographic formula)	
A-sites	
(Nd(1)/Ca(1))-O(1) 2.985(4)	(Nd(1)/Ca(1))-O(3) 2.436(3)
(Nd(1)/Ca(1))-O(1) 2.682(3)	(Nd(1)/Ca(1))-O(3) 2.356(3)
(Nd(1)/Ca(1))-O(1) 2.323(3)	(Nd(1)/Ca(1))-O(3) 3.460(3)
(Nd(1)/Ca(1))-O(1) 3.869 (3)	(Nd(1)/Ca(1))-O(3) 3.693(3)
(Nd(1)/Ca(1))-O(2) 2.846(4)	
(Nd(1)/Ca(1))-O(2) 2.340(3)	
(Nd(1)/Ca(1))-O(2) 2.776(3)	
(Nd(1)/Ca(1))-O(2) 3.835(3)	
Average <*A*-O> = 2.590	BVS(*A*) = 2.2 (should be 2.9)
B'-sites	*B''*-sites
(Ca(2)/Nd(2))-O(1) 2.299(3) x 2	Sn-O(1) 2.078(3) x 2
(Ca(2)/Nd(2))-O(2) 2.291(2) x 2	Sn-O(2) 2.028(2) x 2
(Ca(2)/Nd(2))-O(3) 2.299(2) x 2	Sn-O(3) 2.045(2) x 2
Average <*B'*-O> = 2.296	Average <*B''*-O> = = 2.050
BVS(*B'*) = 2.5 (should be 2.1)	BVS(Sn) = 4.0 (should be 4.0)

Table 3. Selected bond angles (°) for Nd_2CaSnO_6.

$([Nd_{1.90(2)}Ca_{0.10(2)}]_A[Nd_{0.10(2)}Ca_{0.90(2)}]_{B'}[Sn_{1.00}]_{B''}O_6$ crystallographic formula)			
A-sites : (Nd(1)/Ca(1)) in eight coordination		*B'*-sites : (Ca(2)/Nd(2))	*B''*-sites : Sn
O(1)-A-O(2) 61.31(2)	O(1)-A-O(3) 63.68(2)	O(1)-B'-O(2) 89.85(2)	O(1)-Sn-O(2) 88.44(2)
O(1)-A-O(2) 68.52(2)	O(1)-A-O(3) 74.99(2)	O(1)-B'-O(2) 90.14(2)	O(1)-Sn-O(2) 91.56(2)
O(1)-A-O(2) 69.15(2)	O(1)-A-O(3) 77.43(2)	O(1)- B'-O(3) 85.94(2)	O(1)-Sn-O(3) 89.29(2)
O(1)-A-O(2) 71.93(2)	O(2)-A-O(3) 66.15(2)	O(1)-B'-O(3) 94.50(2)	O(1)-Sn-O(3) 90.70(2)
O(1)-A-O(2) 78.39(2)	O(2)-A-O(3) 67.07(2)	O(2)-B'-O(3) 85.96(2)	O(2)-Sn-O(3) 89.10(2)
O(1)-A-O(2) 82.64(2)	O(2)-A-O(3) 72.18(2)	O(2)-B'-O(3) 94.04(2)	O(2)-Sn-O(3) 90.89(2)
O(1)-A-O(1) 76.49(2)	O(2)-A-O(2) 75.20(2)		
O(3)-A-O(3) 88.25(2)			

Table 4. Powder diffraction data of Nd_2CaSnO_6 (CuKα_1; 1.54060 Å). Diffraction lines with $I_{obs.}$ < 1 are omitted.

hkl	$d_{obs.}$(Å)	100 I/I_0	hkl	$d_{obs.}$(Å)	100 I/I_0
011	4.8004	10	024	1.6842	8
-101	4.6596	4	-204	1.6601	4
101	4.6507	8	204	1.6569	5
002	4.0941	06	-312	1.6469	1
110	4.0923	07	312	1.6445	1
-111	3.6627	10	-214	1.5947	1
111	3.6584	11	214	1.5918	1
222	3.0520	9	-213	1.5891	1
020	2.9627	25	-133	1.5402	3
-112	2.8965	84	133	1.5393	4
112	2.8922	100	041	1.4577	5

200	2.8293	27	-224	1.4482	5
021	2.7860	7	224	1.4461	5
-121	2.5001	2	141	1.4115	4
121	2.4988	1	-215	1.3763	2
103	2.4564	2	314	1.3460	1
-211	2.4387	5	-331	1.3459	1
211	2.4361	3	331	1.3452	1
022	2.4002	1	-241	1.2960	1
-202	2.3298	1	241	1.2956	1
202	2.3254	2	-116	1.2952	2
-113	2.2723	3	-332	1.2947	1
113	2.2692	3	116	1.2941	1
-122	2.2106	1	332	1.2936	1
122	2.2087	1	420	1.2766	1
004	2.0471	29	-225	1.2764	2
220	2.0461	30	-135	1.3757	1
023	2.0074	04	-206	1.3756	1
-221	1.9858	05	135	1.3748	1
221	1.9844	05	-243	1.1832	4
-123	1.8928	1	243	1.1823	7
123	1. 8910	2	404	1.1627	12
-213	1.8663	2	-151	1.1485	13
130	1.8648	3	151	1.1484	2
213	1.8629	2	017	1.1473	1
-131	1.8185	9	-136	1.1017	1
131	1.8180	9	316	1.0859	3
311	1.7548	1	027	1.0854	3
-132	1.6975	9	-316	1.0853	1
132	1.6966	9			

Conclusion

The Rietveld refinement, using XRD powder patterns, of Nd_2CaSnO_6 shows clearly that this compound adopts the $P2_1/n$ monoclinic space group. The structure shows that Neodymium and Calcium are divided between the A and B-sites of the ABO_3 perovskite structure. Obtained cationic distribution can be illustrated by the $[Nd_{1.90}Ca_{0.10}]_A[Nd_{0.10}Ca_{0.90}]_{B'}$-$[Sn_{1.00}]_{B''}O_6$ crystallographic formula. Monoclinic structure contains distorted coordination polyhedral of A-site ions, and it is achieved with lower coordination than 12, estimated from the A-O distances. In fact, two groups of distances for A–O lengths are clear, belonging to first (i.e., A-O distances from 2.32 to 2.98 Å) and to the second spheres coordination (i.e., A-O distances from 3.46 to 3.89 Å). The small difference between Calcium and Neodymium ion sizes, respectively in the octahedral (i.e., B-sites) and the eight coordination A-sites, appears to be the driving force of the cationic distribution obtained within the A and B sites of the Nd_2CaSnO_6 perovskite. It appears that the obtained structure distortion results from long-range ordering between Sn in 2c (0 ½ 0) sites and (Ca/Nd) (2) in 2d (1/2 0 0) sites all in the B-sites. Cationic ordering distribution observed for atoms in the B-sites may be related to the difference between their ionic radii (i.e., 0.998 Å for (Ca^{2+}/Nd^{3+}) (2) and 0.69 Å for Sn^{4+}) rather than that between their cationic charge.

References

1- W.E. Pickett and D.J. Singh, Electronic structure and half-metallic transport in the $La_{1-x}Ca_xMnO_3$ system, Phys. Rev. B, **1996**, 53, 1146.

2- K.I. Kobayashi, T Kimura., H. Sawada, K. Terakura and Y. Tokura, Room-temperature magnetoresistance in an oxide material with an ordered double-perovskite structure, Nature, **1998**, 395, 677-680.

3- R.J. Cava, B. Batlogg, J.J. Krajewski, R. Farrow, L.W. Rupp, A.E. White, K. Short, W.F. Peck and T. Kometani, Superconductivity near 30 K without copper: The $Ba_{0.6}K_{0.4}BiO_3$ perovskite, Nature, **1988**, 332, 814-816.

4- J.B. Goodenough, J.M. Longo, in: Landolt-Börnstein. Numerical Data and Functional Relationships in Science and Technology, New Series, Group III: Crystal and Solid State Physics. Vol. 4: Magnetic and Other Properties of Oxides and Related Compounds, Part a, Springer, Berlin, **1970**, p. 126.

5- P.D. Battle, T.C. Gibb, C.W. Jones and F. Studer, The crystal and magnetic structures of Ca_2NdRuO_6, Ca_2HoRuO_6, and Sr_2ErRuO_6, J. Solid State Chem., **1989**, 78,281-293.

6- C.R. Wiebe, J.E. Greedan, P.P. Kyriakou, G.M. Luke, J.S. Gardner, A. Fukaya, I.M. Gat-Malureanu, P.L. Russo, A.T. Savici and Y.J. Uemura, Frustration-driven spin freezing in

the S=12 fcc perovskite Sr_2MgReO_6 , Phys. Rev. B, **2003**, 68, 134410.

7- M.T. Anderson, K, B greenwood, G A. Taylor and K.R. Poeppelmeier, Prog. B-cation arrangements in double perovskites, J. Solid State Chem., **1993**, 22, 197-233.

8- M. R. Palacin, J. Bassas, J. Rodriguez-Carvajal and P. Gomez-Romero, Syntheses of the Perovskite La_2CuTiO_6 by the Ceramic, Oxide Precursors and Sol-Gel methods. Study of the structure and the Cu-Ti Distribution by X-Ray and Neutron Diffraction, J. Mater. Chem., **1993**, 3(1l), 1171-1177.

9- R. Ubic, Y. Hu and I. Abrahams, Neutron and electron diffraction studies of $La(Zn_{1/2}Ti_{1/2})O_3$ perovskite, Acta Crystallogr. B, **2006**, 62, 521–529.

10- M. Avdeev, M. P. Seabra and V. M. Ferreira, Crystal Structure of Dielectric Ceramics in the $La(Mg_{0.5}Ti_{0.5})O_3$-$BaTiO_3$ System, J. Mater. Res., **2002**, 17, 1112–1117.

11- W. A. Groen, F. P. F. Van Berkel and D. J. W. Ijdo, Dineodymium magnesium titanate (IV). A Rietveld refinement of neutron Powder diffraction data, Acta Crystallogr .C, **1986**, 42, 1472-1475.

12- M. Azuma, S. Kaimori and M. Takano, High-Pressure Synthesis and Magnetic Properties of Layered Double Perovskites Ln_2CuMO_6 (Ln = La, Pr, Nd, and Sm; M = Sn and Zr), J. Chem. Mater, **1998**, 10, 3124-3130.

13- Anderson M. T and Poeppelmeier K. R., Lanthanum copper tin oxide (La_2CuSnO_6): a new perovskite-related compound with an unusual arrangement of B cations, Chem. Mater., **1991**, 3, 476-482.

14- C. Sakai, Y. Doi and Y. Hinatsu, Crystal structures and magnetic properties of double perovskite compounds Ca_2LnRuO_6 (Ln = Y, La–Lu), J. Alloy Compd., **2006**, 408, 608-612

15- X. Yin, Y. Wang, F. Huang, Y. Xia, D. Wan and J. Yao, Excellent red phosphors of double perovskite Ca_2LaMO_6: Eu (M= Sb, Nb, Ta) with distorted coordination environment, J. Solid State Chem., **2011**, 184, 3324–3328.

16- A. Faik, I. Urcelay, E. Iturbe-Zabalo and J. M. Igartua, Cationic ordering and role of the A-site cation on the structure of the new double perovskites $Ca_{2-x}Sr_xRSbO_6$ R=La, Sm and (x=0,0.5,1), J. Mol. Struct., **2010**, 977, 137-144.

17- S. Halder, Md. Sariful Sheikh, B. Ghosh and T.P. Sinha, Octahedral distortion induced phonon vibration and electrical conduction in A $_2NdSbO_6$

(A = Ba, Sr, Ca), J. Mater. Chem. Phys., **2017**, 199, 508-521.

18- A. Aatiq, Synthesis and crystal structure of the new perovskite $CaLa_2CaTi_2O_9$ (= $(Ca_{1/3}La_{2/3})_A(Ca_{1/3}Ti_{2/3})_BO_3$), Solid State Sci. , **2003**, 5, 745-749.

19- A. Aatiq and A. Boukhari, Synthesis and structural study of the new perovskite series $CaLn_2ZnTi_2O_9$ (= $(Ca_{1/3}Ln_{2/3})_A(Zn_{1/3}Ti_{2/3})_BO_3$) (Ln=La, Pr, Nd, Eu), Mater. Lett., **2004**, 58, 2406–2411.

20- E. Iturbe-Zabalo, J.M. Igartua, A. Aatiq, and V. Pomjakushin, A structural study of the $CaLn_2CuTi_2O_9$ (Ln = Pr, Nd, Sm) and $BaLn_2CuTi_2O_9$ (Ln =La, Pr, Nd) triple perovskite series, J. Mol. Struct., **2013**, 1034, 134–143.

21- J. Rodriguez-Carvajal, Recent advances in magnetic structure determination by neutron powder diffraction, Physica B: Condensed Matter., **1993**, 192, 55-69.

22- S. Geller, Crystal Structure of Gadolinium Orthoferrite $GdFeO_3$, J. Chem. Phys., **1956,** 24, 1236-1239.

23- I. Levin, L.A. Bendersky, J.P. Cline, R.S. Roth and T.A. Vanderah, Octahedral Tilting and Cation Ordering in Perovskite-Like $Ca_4Nb_2O_9$=3•$Ca(Ca_{1/3}Nb_{2/3})O_3$ Polymorphs, J. Solid State Chem., **2000**, 150, 43-61.

24- I. Levin, J.Y. Chan, R.G. Geyer, J.E. Maslar and T.A. Vanderah, Cation Ordering Types and Dielectric Properties in the Complex Perovskite $Ca(Ca_{1/3}Nb_{2/3})O_3$, J. Solid State Chem. , (**2001**), 156 ,122-134.

25- R.D. Shannon Revised effective ionic radii and systematic studies of interatomic distances in halides and chalcogenides, Acta Crystallogr. A, **1976**, 32,751-767.

26- V. M. Goldschmidt, Die Gesetze der Krystallochemie, J. Die Naturwissenschaften., **1926**, 14, 477-485.

27- I.D. Brown and D. Altermatt, Bond-valence parameters obtained from a systematic analysis of the Inorganic Crystal Structure Database , Acta Crystallogr. B, **1985**, 41, 244-247.

28- P.W.Barnes, M. W. Lufaso and P. M. Woodward, Structure determination of $A_2M^{3+}TaO_6$ and $A_2M^{3+}NbO_6$ ordered perovskites: octahedral tilting and pseudo symmetry , Acta Crystallogr. B, **2006**, 62, 384-396.

29- P. Woodward, R.D. Hoffmann and A.W. Sleight, Order–disorder in $A_2M^{3+}M^{5+}O_6$ Perovskites, J. Mater. Res., **1994**, 9, 2118-2127.